

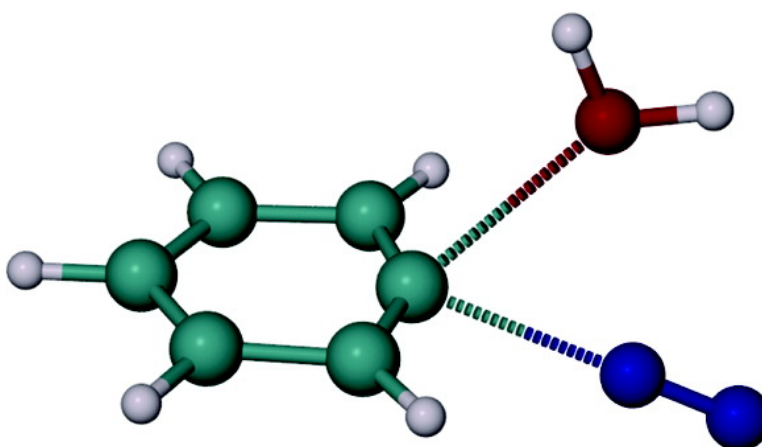
Article

Ab Initio Study of the S₁Ar and S₂Ar Reactions of Benzenediazonium Ion with Water. On the Conception of “Unimolecular Dediazonation” in Solvolysis Reactions

Zhengyu Wu, and Rainer Glaser

J. Am. Chem. Soc., **2004**, 126 (34), 10632-10639 • DOI: 10.1021/ja047620a • Publication Date (Web): 06 August 2004

Downloaded from <http://pubs.acs.org> on April 1, 2009



More About This Article

Additional resources and features associated with this article are available within the HTML version:

- Supporting Information
- Links to the 2 articles that cite this article, as of the time of this article download
- Access to high resolution figures
- Links to articles and content related to this article
- Copyright permission to reproduce figures and/or text from this article

[View the Full Text HTML](#)



ACS Publications
High quality. High impact.

Ab Initio Study of the S_N1Ar and S_N2Ar Reactions of Benzenediazonium Ion with Water. On the Conception of “Unimolecular Dediazonation” in Solvolysis Reactions

Zhengyu Wu and Rainer Glaser*

Contribution from the Department of Chemistry, University of Missouri—Columbia, Columbia, Missouri 65211

Received April 24, 2004; E-mail: glaser@missouri.edu

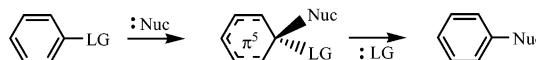
Abstract: The nucleophilic substitution of N₂ in benzenediazonium ion **1** by one H₂O molecule to form protonated phenol **2** has been studied with ab initio (RHF, MP2, QCISD(T)/MP2) and hybrid density functional (B3LYP) methods. Three mechanisms were considered: (a) the unimolecular process S_N1Ar with steps **1** → Ph⁺ + N₂ and Ph⁺ + H₂O → **2**, (b) the bimolecular process S_N2Ar with precoordination **1** + H₂O → **1**·H₂O, S_N reaction **1**·H₂O → [TS][‡] → **2**·N₂ and dissociation of the postcoordination complex **2**·N₂ → **2** + N₂, and (c) the direct bimolecular process S_N2Ar that bypasses precoordination and involves just the S_N reaction **1** + H₂O → [TS][‡] → **2** + N₂. The S_N2Ar reactions proceed by way of a C_s symmetric S_N2Ar transition state structure that is rather loose, contains essentially a phenyl cation weakly bound to N₂ and OH₂, and is analogous to the transition state structures of front-side nucleophilic replacement at saturated centers. In solvolysis reactions, all of these processes follow first-order kinetics, and the electronic relaxation is essentially the same. It is argued that “unimolecular dediazonations” have to proceed by way of S_N2Ar transition state structures because strict S_N1Ar reactions cannot be realized in solvolyses, despite the fact that the Gibbs free energy profile favors the strict S_N1Ar process over the S_N2Ar reaction by 6.7 kcal/mol. It is further argued that the direct S_N2Ar process is the best model for the solvolysis reaction for dynamic reasons, and its Gibbs free energy of activation is 19.3 kcal/mol and remains higher than the S_N1Ar value. Even though the S_N1Ar and S_N2Ar models provide activation enthalpies and SKIE values that closely match the experimental data, the analysis leads us to the unavoidable conclusion that this agreement is fortuitous. While the experiments do show that the solvent effect on the activation energy is about the same for all solvents, they do not show the absence of a solvent effect. The ab initio results presented here suggest that the solvent effect on the direct S_N2Ar dediazonation is approximately 12 kcal/mol, and computation of solvent effects with the isodensity polarized continuum model (IPCM) support this conclusion.

Introduction

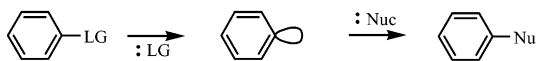
The usual mechanism for nucleophilic aromatic substitution is the addition–elimination pathway, denoted S_NAr-Ad,E or S_N2 and called the “bimolecular mechanism”, and this involves the bimolecular formation of the Meisenheimer σ-complex¹ as an intermediate (Scheme 1). The reverse sequence, the elimination–addition pathway, denoted S_NAr-E,Ad or simply S_N1, is more rare and it is referred to as the “unimolecular mechanism”.² This nomenclature implies that the elimination is essentially complete at the time of the addition of the incoming nucleophile. This reaction mechanism is the aromatic equivalent of the unimolecular nucleophilic substitution at sp³ centers and is best denoted as S_N1Ar. However, there is a third option, and this third option is the bimolecular process in which the elimination of the leaving group and the addition of the nucleophile occur more or less simultaneously and without formation of an

Scheme 1. Mechanisms of Nucleophilic Aromatic Substitution

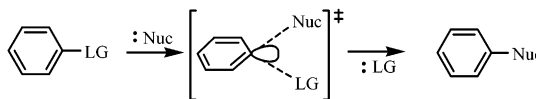
S_NAr-Ad,E (Addition-Elimination)



S_NAr-E, Ad (Elimination-Addition) or S_N1Ar



S_N2Ar Bimolecular Pathway



intermediate. This reaction is the aromatic equivalent of the front-side bimolecular nucleophilic substitution at sp³ centers. We denote this reaction mechanism as S_N2Ar. The intermediate of the S_NAr-Ad,E process and the transition state structure of the S_N2Ar mechanism are topologically the same, but they differ

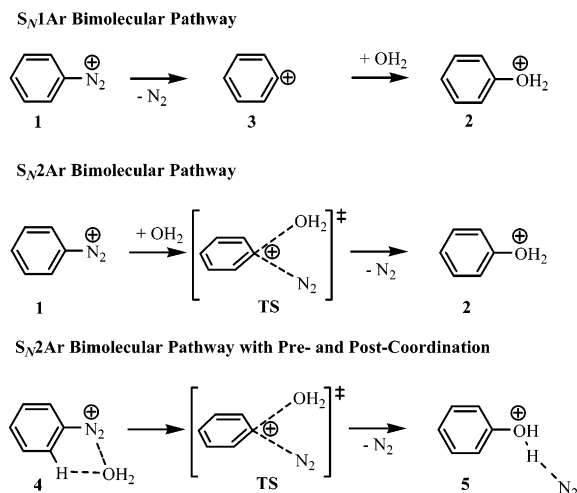
(1) (a) Bernasconi, C. F. *Acc. Chem. Res.* **1978**, *11*, 147. (b) Paradisi, C. In *Comprehensive Organic Synthesis*; Trost, B. M., Fleming, I., Ed.; Pergamon Press: Oxford, 1991; Vol. 4, p 423.
 (2) (a) Miller, J. *Aromatic Nucleophilic Substitution*; Elsevier: London, 1968.
 (b) Ross, S. D. *Prog. Phys. Org. Chem.* **1963**, *1*, 31.
 (3) Behr, J. P. *J. Chem. Soc., Chem. Commun.* **1989**, 101.

in the C–nucleophile (C–Nuc) and C–leaving group (C–LG) bonds. Both of these bonds have to be short in the intermediate; while one can imagine the S_N2Ar mechanism to involve two partial bonds, and both could be very weak (essentially free cation intermediate, S_N1Ar -like) or relatively strong (most like in the aliphatic S_N2 reaction) or unsymmetrical (early or late S_N2Ar). The S_N2Ar mechanism with an essentially broken C–LG bond and a barely formed C–Nuc bond would be rather S_N1Ar -like, and in terms of geometry and experimentally, one would not be able to differentiate between these two mechanisms if the nucleophile is used in excess (solvolysis).

We are interested in two types of deamination reactions and these are (I) the deamination of aliphatic and aromatic amines and their role in the alkylation or arylation of DNA and (II) the deamination of the amino groups of the DNA bases in nucleic acids. Aromatic diazonium ions are important in both of the processes I and II, and they both have significance in chemical toxicology. Arenediazonium ions are implicated in DNA arylations that may proceed via the phenyl cation³ or radical.⁴ The study of aromatic diazonium ions also is central to the understanding of the heteroaromatic diazonium ions relevant to DNA base deamination.^{5,6} The mechanism of the dediazonation reaction of benzenediazonium ion (**1**) has been studied extensively.⁷ The conventional consensus holds that dediazonation reactions follow an S_N1 -like mechanism, because of the low selectivity among nucleophiles.^{8,9} Lewis et al.¹⁰ and Swain et al.¹¹ studied the kinetics of the reactions of **1** in aqueous solution. Their experimental results provided evidence that the dediazonation reaction of **1** proceeds via a highly reactive phenyl cation. Further experimental and theoretical studies by Zollinger et al. demonstrated that the nucleophilic substitution proceeds through the phenyl cation intermediate and suggested that the phenyl cation might be free or solvent-separated from nitrogen.¹²

We have been studying benzenediazonium ion with physical and theoretical organic methods. Our theoretical studies of the electron density distributions of diazonium ions led to a new bonding model¹³ that emphasizes dative bonding between the phenyl cation and an overall essentially neutral N_2 group.¹⁴ Hence, the phenyl cation already exists in the “diazonium” ion

Scheme 2. S_N1Ar and S_N2Ar Reaction of Water with Benzenediazonium Ion



and little electron density relaxation occurs during dediazonation.¹⁵ Here, we are reporting on the replacement of dinitrogen in benzenediazonium ion by one water molecule and we present a comparison of the S_N1Ar and S_N2Ar processes (Scheme 2), including computed solvation effects. Cuccovia et al. recently reported results of both experimental and theoretical studies (RHF) on the reaction rate constant of the benzenediazonium ion dediazonation.¹⁶ Their conclusion was that in the gas phase and aqueous solution the reaction is dominated by a bimolecular pathway and in a low polarity solvent the reaction is dominated by a unimolecular pathway.

Theoretical Methods

Ab initio and density functional calculations were carried out with Gaussian98^{17,18} on two clusters of Compaq Alphaservers ES40 and ES45. Geometries were optimized within the redundant internal coordinates and started with C_1 symmetry. We indicate all the symmetry changes, e.g. C_1 to C_s , if any. Harmonic vibrational frequencies were determined analytically for all stationary structures. Optimization and thermodynamical analyses were carried out at the RHF level, with the inclusion of dynamic electron correlation at the MP2(full) level, as well as with density functional theory¹⁹ using the hybrid method Becke3LYP.²⁰ The 6-31G** basis set was used in all cases. When questions remained

- (4) (a) Griffiths, J.; Murphy, J. A. *J. Chem. Soc., Chem. Commun.* **1992**, 24. (b) Arya, D. P.; Warner, P. M.; Jebaratnam, D. *J. Tetrahedron Lett.* **1993**, 34, 7823.
 (5) (a) Glaser, R.; Son, M.-S. *J. Am. Chem. Soc.* **1996**, 118, 10942. (b) Glaser, R.; Rayat, S.; Lewis, M.; Son, M.-S.; Meyer, S. *J. Am. Chem. Soc.* **1999**, 121, 6108. (c) Hodgen, B.; Rayat, S.; Glaser, R. *Org. Lett.* **2003**, 5, 4077. (d) Rayat, S.; Wu, Z.; Glaser, R. *Chem. Res. Toxicol.* **2004**, 17, xxx.
 (6) (a) Qian, M.; Glaser, R. *J. Am. Chem. Soc.* **2004**, 126, 2274. (b) Rayat, S.; Majumdar, P.; Tipton, P.; Glaser, R. *J. Am. Chem. Soc.* **2004**, 126, xxx.
 (7) Zollinger, H. *Diazo Chemistry I*; VCH Publications: New York, 1994.
 (8) *The Chemistry of the Diazonium and Diazo Groups*; Patai, S., Ed.; John Wiley & Sons: New York, 1978.
 (9) Saunders, K. H.; Allen, R. L. M. *Aromatic Diazo Compounds*, 3rd ed.; Edward Arnold: Baltimore, MD, 1985.
 (10) (a) Lewis, E. S.; Insole, J. M. *J. Am. Chem. Soc.* **1964**, 86, 34. (b) Lewis, E. S.; Cooper, J. E. *J. Am. Chem. Soc.* **1962**, 84, 3847. (c) Lewis, E. S. *J. Am. Chem. Soc.* **1958**, 80, 1371.
 (11) (a) Swain, C. G.; Sheats, J. E.; Harbison, K. G. *J. Am. Chem. Soc.* **1975**, 97, 783. (b) Swain, C. G.; Sheats, J. E.; Gorenstein, D. G.; Harbison, K. G. *J. Am. Chem. Soc.* **1975**, 97, 791. (c) Swain, C. G.; Rogers, R. J. *J. Am. Chem. Soc.* **1975**, 97, 799.
 (12) (a) Szele, I.; Zollinger, H. *J. Am. Chem. Soc.* **1978**, 100, 2811. (b) Hashida, Y.; Landells, R. G. M.; Lewis, G. E.; Szele, I.; Zollinger, H. *J. Am. Chem. Soc.* **1978**, 100, 2816. (c) Gamba, A.; Sinonetta, M.; Suffritti, G.; Szele, I.; Zollinger, H. *J. Chem. Soc., Perkin Trans. 2*, **1980**, 493.
 (13) (a) Glaser, R.; Choy, G. S.-C.; Hall, M. K. *J. Am. Chem. Soc.* **1991**, 113, 3, 1109–1120. (b) Glaser, R.; Choy, G. S.-C. *J. Am. Chem. Soc.* **1993**, 115, 2340–2347. (c) Horan, C. J.; Glaser, R. *J. Phys. Chem.* **1994**, 98, 3989–3992.
 (14) Glaser, R.; Horan, C. J. *J. Org. Chem.* **1995**, 60, 7518.

- (15) (a) Glaser, R.; Horan, C. J.; Lewis, M.; Zollinger, H. *J. Org. Chem.* **1999**, 64, 902. (b) Glaser, R.; Horan, C. J.; Zollinger, H. *Angew. Chem.* **1997**, 109, 2324. *Angew. Chem., Int. Ed. Engl.* **1997**, 36, 2210.
 (16) Cuccovia, I. M.; Silva, M. A.; Ferraz, H. M. C.; Pliego, J. R.; Riveros, J. M.; Chaimovich, H. *J. Chem. Soc., Perkin Trans. 2*, **2000**, 1986.
 (17) Frisch, M. J.; Trucks, G. W.; Schlegel, H. B.; Scuseria, G. E.; Robb, M. A.; Cheeseman, J. R.; Zakrzewski, V. G.; Montgomery, J. A.; Stratmann, R. E.; Burant, J. C.; Dapprich, S.; Millam, J. M.; Daniels, A. D.; Kudin, K. N.; Strain, M. C.; Farkas, O.; Tomasi, J.; Barone, V.; Cossi, M.; Cammi, R.; Mennucci, B.; Pomelli, C.; Adamo, C.; Clifford, S.; Ochterski, J.; Petersson, A.; Ayala, P. Y.; Cui, Q.; Morokuma, K.; Malick, D. K.; Rabuck, A. D.; Raghavachari, K.; Foresman, J. B.; Cioslowski, J.; Ortiz, J. V.; Stefanov, B. B.; Liu, G.; Liashenko, A.; Piskorz, P.; Komaromi, I.; Gomperts, R.; Martin, R. L.; Fox, D. J.; Keith, T.; Al-Laham, M. A.; Peng, C. Y.; Nanayakkara, A.; Gonzalez, C.; Challacombe, M.; Gill, P. M. W.; Johnson, B. G.; Chen, W.; Wong, M. W.; Andres, J. L.; Head-Gordon, M.; Replogle, E. S.; Pople, J. A. *Gaussian 98, Revision A.1*; Gaussian, Inc., Pittsburgh, PA, 1998.
 (18) Cramer, C. J. *Essentials of Computational Chemistry*; John Wiley & Sons: New York, 2002.
 (19) (a) March, N. H. *Electron Density Theory of Atoms and Molecules*; Academic Press: San Diego, CA, 1992. (b) Labanowski, J. K.; Andzelm, J. W.; Eds. *Density Functional Methods in Chemistry*; Springer-Verlag: New York, 1991. (c) Parr, R. G.; Yang, W. *Functional Theory of Atoms and Molecules*; Oxford University Press: New York, 1989.
 (20) (a) Becke, A. D. *Phys. Rev. A* **1986**, 33, 2786. (b) Becke, A. D. *J. Chem. Phys.* **1988**, 88, 2547. (c) Lee, C.; Yang, W.; Parr, R. G. *Phys. Rev. B* **1988**, 37, 785.

Table 1. Pertinent Relative Energies, Reaction Energy, and Activation Energies^a

	RHF			MP2(full)		
	ΔE	ΔH	ΔG	ΔE	ΔH	ΔG
$1 \rightarrow \text{Ph}^+ + \text{N}_2$	25.3	20.8	9.7	39.3	34.5	23.1
$\text{Ph}^+ + \text{H}_2\text{O} \rightarrow \mathbf{2}$	-55.0	-49.7	-38.3	-59.9	-54.5	-43.1
$1 + \text{H}_2\text{O} \rightarrow \mathbf{1}\cdot\text{H}_2\text{O}$	-12.7	-10.5	-2.6	-14.9	-12.7	-4.6
$1 + \text{H}_2\text{O}$ vs TS	10.7	9.4	13.3	19.3	18.1	23.9
$\mathbf{1}\cdot\text{H}_2\text{O}$ vs TS	23.3	19.9	15.9	34.2	30.8	28.5
$1 + \text{H}_2\text{O} \rightarrow \mathbf{2} + \text{N}_2$	-29.7	-28.9	-28.7	-20.7	-20.2	-20.0
	QCISD(T)/MP2(full)			B3LYP		
	ΔE	ΔH	ΔG	ΔE	ΔH	ΔG
$1 \rightarrow \text{Ph}^+ + \text{N}_2$	33.1	28.3	16.9	37.4	32.7	21.5
$\text{Ph}^+ + \text{H}_2\text{O} \rightarrow \mathbf{2}$	-56.6	-51.2	-39.7	-56.5	-51.2	-39.8
$1 + \text{H}_2\text{O} \rightarrow \mathbf{1}\cdot\text{H}_2\text{O}$	-14.5	-12.3	-4.2	-13.7	-11.5	-3.5
$1 + \text{H}_2\text{O}$ vs TS	14.8	13.6	19.3	20.1	19.1	24.7
$\mathbf{1}\cdot\text{H}_2\text{O}$ vs TS	29.3	25.9	23.6	33.8	30.6	28.2
$1 + \text{H}_2\text{O} \rightarrow \mathbf{2} + \text{N}_2$	-23.5	-23.0	-22.8	-19.1	-18.5	-18.4
	QCISD(T)/MP2(full) ^c					
	ΔE	ΔH	ΔG			
$1 \rightarrow \text{Ph}^+ + \text{N}_2$	34.8	30.0	18.6			
$\text{Ph}^+ + \text{H}_2\text{O} \rightarrow \mathbf{2}$	-57.9	-52.5	-41.0			
$1 + \text{H}_2\text{O}$ vs TS	16.3	15.1	20.8			
$1 + \text{H}_2\text{O} \rightarrow \mathbf{2} + \text{N}_2$	-23.1	-22.6	-22.4			

^a All data in kcal/mol. ^b Unless specified otherwise, the calculations employed the 6-31G** basis set. ^c Using the 6-311G(2df,p) basis set in the QCISD(T) calculation.

as to the quality of the correlation treatment, we performed single-point energy calculations at the QCISD(T)/6-31G** and QCISD(T)/6-311G(2df,p) levels,²¹ and all QCISD(T) energies were computed for the MP2/6-31G**-optimized structures. Total energies are provided in Supporting Information.

Relative energies are reported in Table 1 and they all are relative to the sum of the energies of isolated benzenediazonium ion and water. Besides the electronic energy (ΔE), we also determined the enthalpy (ΔH) and the free energy (ΔG). Because we are modeling the reaction in solution, RT was not included in the calculation of ΔH to exclude the gas-phase volume effect. Therefore, $\Delta H = \Delta E_{298}$, where ΔE_{298} is the sum of ΔE and thermal energy correction at 298 K. ΔG was calculated with ΔH in conjunction with $T\Delta S$ for standard conditions (1 atm, 298 K). Thermal corrections to the QCISD(T) energies are based on the MP2 data. All activation parameters are determined as the difference between the transition state and the reactants. In the case of the $S_N1\text{Ar}$ and the direct $S_N2\text{Ar}$, the reactants are $\mathbf{1}$ and water, and in the case of the (indirect) $S_N2\text{Ar}$, the reactant is the precoordination complex.

The secondary kinetic isotope effects²² (SKIE) were determined at the MP2/6-31G** level via the equation $k_H/k_D = \exp((\Delta G_D^\ddagger - \Delta G_H^\ddagger)/RT)$, which is deduced from the combination of the Eyring equation $k = (\kappa T/h)\exp(-\Delta G^\ddagger/RT)$ where κ is the Boltzmann constant.

Solvation effects on energies were examined with the isodensity surface polarized continuum model (ICPM) by Foresman et al. at the MP2/6-31G** level.^{23,24} Total energies computed with the ICPM model are provided as part of the Supporting Information, and Table 2 summarizes the solvation effects on pertinent reaction energies.

Table 2. Secondary Kinetic Isotope Effects of the Reaction of Benzenediazonium Ion with Water^a

deuteration	$S_N1\text{Ar}$		direct $S_N2\text{Ar}$		expl ^c k_H/k_D
	ΔG^\ddagger ^b	k_H/k_D	ΔG^\ddagger ^b	k_H/k_D	
none	23.11		23.89		
2-d	23.23	1.22	23.97	1.15	1.22
3-d	23.17	1.11	23.93	1.07	1.08
4-d	23.11	1.01	23.89	1.01	1.02

^a At MP2(full)/6-31G**. ^b Reaction activation free energy in kcal/mol. ^c Ref 44.

Results and Discussion

Unimolecular Hydrolysis of Benzenediazonium Ion. Hydrolysis of Benzenediazonium Ion. The optimized structures of benzenediazonium ion ($\mathbf{1}$) and phenyl cation ($\mathbf{3}$) are shown in Figure 1. Both the structures of $\mathbf{1}$ and $\mathbf{3}$ are C_{2v} symmetric. The structural data of $\mathbf{1}$ are in excellent agreement with the available solid-state salts PhN_2^+X^- ($\text{X}^- = \text{Cl}^-, \text{Br}_3^-, \text{BF}_4^-$).²⁵ Structures of loosely coordinated phenyl cations have been characterized recently by solid-state NMR spectroscopy by Frohn et al.²⁶ Also very recently, Winkler and Sander isolated phenyl cation in a solid argon matrix and confirmed that the ground state of $\mathbf{3}$ is a 1A_1 singlet.²⁷ Iwata et al. also established firmly that the singlet state is the ground state of phenyl cation based on a high level theoretical study.²⁸ Therefore, the structure of phenyl cation was optimized with singlet multiplicity in the present study.

Kuokkanen studied the decomposition of arenediazonium ions (with and without crown ether complexation) in dichloromethane and reported that the ΔH for the dissociation of $\mathbf{1}$ in solvent mixtures of 1,2-dichloroethane is 25.7 kcal/mol and the ΔG is 23.1 kcal/mol.²⁹ Zollinger et al. studied the decomposition of $\mathbf{1}$ in 2,2,2-trifluoroethanol in the presence or absence of benzene and determined activation energies of 27.7 and 28.3 kcal/mol, respectively.³⁰ In fact, Szele and Zollinger measured the rates of the dediazonation of salts of $\mathbf{1}$ in 19 different solvents and found that the solvent essentially has no influence on the dissociation rate.^{30b,c} The dative bonding model for diazonium ions can explain this experimental observation, and this connection between experiment and theory was an important one to establish.¹⁴ The other important connection between experiment and theory was provided by us and Zollinger with the demonstration that the dative bonding model can provide a physically meaningful explanation of the opposite signs of the reaction constants in dual-parameter Hammett equations for dediazoniations.¹⁵

The dissociation energy is the reaction energy for the dissociation of $\mathbf{1}$ to form singlet phenyl cation ($\mathbf{3}$) and N_2 . We reported a binding energy of $\mathbf{1}$ of 38.6 kcal/mol at the MP2-(full)/6-31G* level and an enthalpy of 32.6 kcal/mol.^{14c} At the MP2(full)/6-31G** level employed in the present study, we find a binding energy for $\mathbf{1}$ of $\Delta E = 39.3$ kcal/mol and $\Delta H = 34.4$

- (21) Pople, J. A.; Head-Gordon, M.; Raghavachari, K. *J. Chem. Phys.* **1987**, *87*, 5968.
 (22) (a) Lowry, T.; Richardson, K. S. *Mechanism and Theory in Organic Chemistry*, 2nd ed.; Harper & Row: Publishers: New York, 1981; p 194. (b) Wiberg, K. B. *Physical Organic Chemistry*; John Wiley & Sons: New York, 1964. (c) Melander, L.; Saunders, W. H. *Reaction Rates of Isotopic Molecules*; John Wiley & Sons: New York, 1980.
 (23) (a) Foresman, J. B.; Keith, T. A.; Wiberg, K. B.; Snoonian, J.; Frisch, M. J. *J. Phys. Chem.* **1996**, *100*, 16098. (b) Pomelli, C. S.; Tomasi, J. *J. Phys. Chem. A* **1997**, *101*, 3561.
 (24) Cramer, C. J.; Truhlar, D. G. *Chem. Rev.* **1999**, *99*, 2161.

- (25) (a) Rømming, C. *Acta Chem. Scand.* **1963**, *17*, 1444. (b) Andresen, O.; Rømming, C. *Acta Chem. Scand.* **1962**, *16*, 1882. (c) Cygler, M.; Przybylska, M.; Eloffson, R. *Can. J. Chem.* **1982**, *60*, 2852.
 (26) Bailly, F.; Barthen, P.; Frohn, H.-J.; Kockerling, M. *Z. Anorg. Allg. Chem.* **2000**, *626*, 2419.
 (27) Winkler, M.; Sander, W. *Angew. Chem., Int. Ed.* **2000**, *39*, 2014.
 (28) Hrusák, J.; Schröder, D.; Iwata, S. *J. Chem. Phys.* **1997**, *106*, 7541.
 (29) (a) Kuokkanen, T.; Virtanen, P. O. I. *Acta Chim. Scand. B* **1979**, *33*, 725. (b) Kuokkanen, T. *Acta Chim. Scand.* **1990**, *44*, 394.
 (30) (a) Burri, P.; Wahl, G. H., Jr.; Zollinger, H. *Helv. Chim. Acta* **1974**, *57*, 2099. (b) Szele, I.; Zollinger, H. *Helv. Chim. Acta* **1978**, *61*, 1721. (c) Lorand, J. P. *Tetrahedron Lett.* **1989**, *30*, 7337.

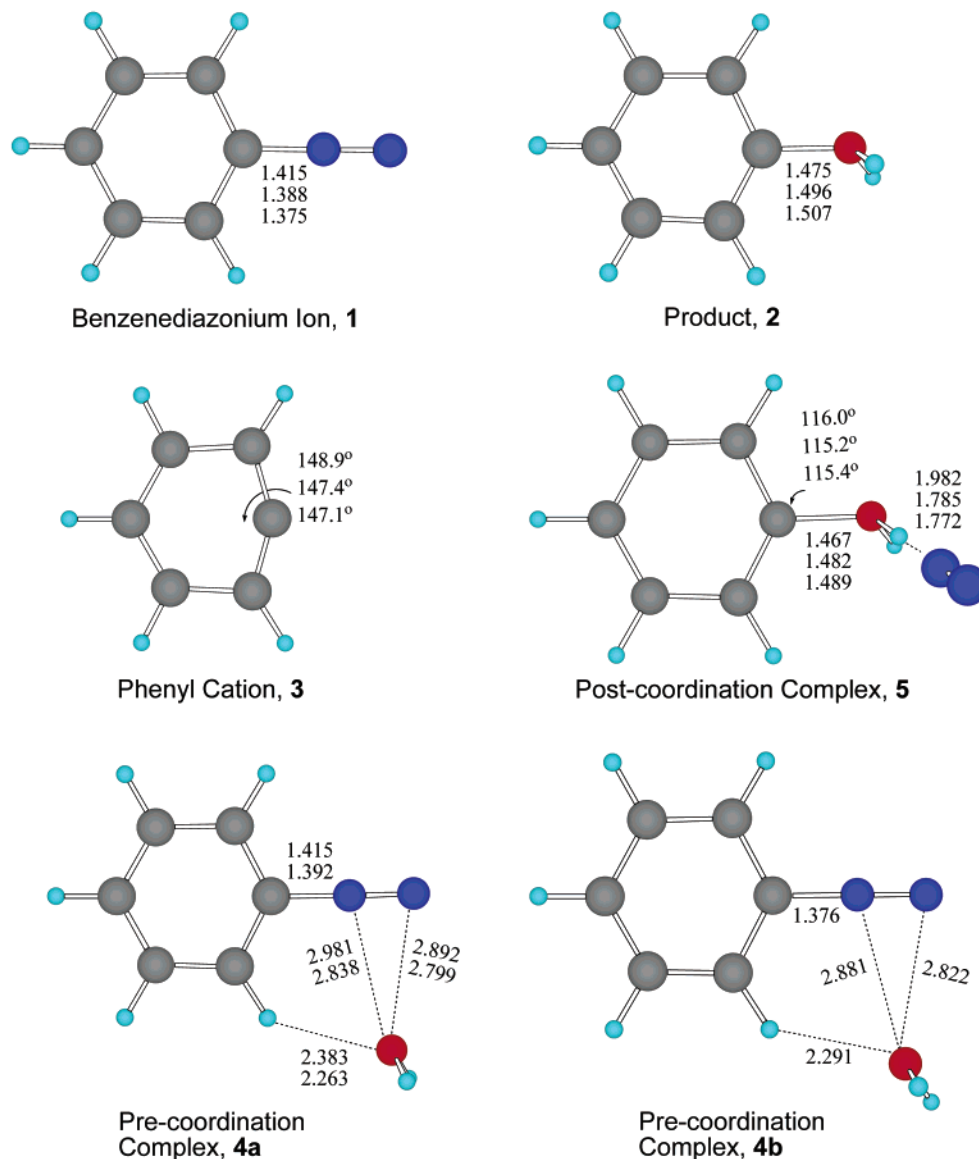


Figure 1. Molecular models of the stationary structures relevant to the benzenediazonium ion hydrolysis reaction. Geometry parameters are listed in the sequence RHF, MP2, and B3LYP. **4a** represents the geometry at RHF and MP2, and **4b** represents the B3LYP geometry.

kcal/mol and $\Delta G = 23.1$ kcal/mol. At the level QCISD(T)/6-31G**//MP2(full)/6-31G**, the dissociation enthalpy is $\Delta H = 28.3$ kcal/mol. An improvement of the basis set causes only small change; $\Delta H = 28.3$ kcal/mol was computed at QCISD(T)/6-311G(2df,p)//MP2(full)/6-31G**. The experimental solution data by Kuokkanen and Zollinger are in excellent numerical agreement with the computed dissociation enthalpies of **1**, and it is because of this agreement that the S_N1Ar mechanism has been discussed. We will show below that this reasoning is not justified. In the following, we refer to the QCISD(T)/6-31G**//MP2(full)/6-31G** data unless otherwise noted.

Water Addition to Phenyl Cation. The reaction enthalpy for the addition of water to phenyl cation is exothermic by 51.2 kcal/mol, and this value is the bond dissociation energy of the C–O bond in **2**. Note that the C–O bond length is 1.47 Å and much longer than that of 1.38 Å in phenol.³¹ If the C–O bond in **2** were a strong covalent bond, most of the positive charge would reside on water. On the other hand, if this C–O bond

were a pure dative bond, most of the positive charge should be located on the phenyl ring. Natural population analysis³² (NPA) shows that the overall charge on the phenyl ring is 0.53 and that on water is 0.47, while in phenol the overall charges on the phenyl ring and the OH group are 0.25 and –0.25, respectively. Hence, there is an electron transfer of about 0.28 e from the phenyl group toward the OH group upon phenol protonation. And the charge distribution within **2** indicates that the C–O bond can be characterized as a partial covalent bond and, consequently, heterolysis is facile.

The optimized structure of **2** (Figure 1) is C_s symmetric with the water H atoms above and below the plane of the benzene ring.³³ This structure is significantly different from that of the isoelectronic aniline. In aniline, both of the amino H atoms are on the same side of the best plane of the molecule, while the N

(31) Gas-phase electron diffraction study: Portalone, G.; Schultz, G.; Domenicani, A.; Hargittai, I. *Chem. Phys. Lett.* **1992**, *197*, 482.

(32) (a) Glendening, E. D.; Reed, A. E.; Carpenter, J. E.; Weinhold, F. *NBO Version 3.1*. (b) Glendening, E. D.; Weinhold, F. *J. Comput. Chem.* **1998**, *19*, 628.

(33) See also: (a) Tishchenko, O.; Pham-Tran, N.-N.; Kryachko, E. S.; Nguyen, M. T. *J. Phys. Chem. A* **2001**, *105*, 8709. (b) DeFrees, D. J.; McIver, R. T.; Hehre, W. J. *J. Am. Chem. Soc.* **1977**, *99*, 3853.

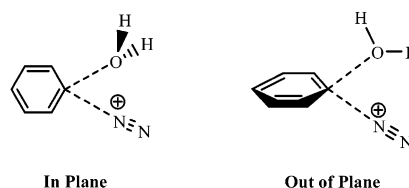
atom is displaced toward the other side; this geometry allows for some interaction between the conjugated π -system and the N lone pair.³⁴ The aniline molecule also is C_s symmetric, but with the symmetry plane perpendicular to the benzene ring. One possible explanation is that due to the extra positive charge of **2**, the electron density of the O lone pair is reduced so much that it cannot effectively interact with the benzene π -system.

Reaction Energy and S_N1Ar Activation Barrier. The S_N1Ar reaction consists of the combination of the unimolecular bond dissociation of **1** and the water addition to the phenyl cation, and this process is exothermic and exergonic with $\Delta E = 23.5$ kcal/mol, $\Delta H = 23.0$ kcal/mol, and $\Delta G = 22.8$ kcal/mol. The activation parameters are $\Delta E^\ddagger = 33.1$ kcal/mol, $\Delta H^\ddagger = 28.3$ kcal/mol, and $\Delta G^\ddagger = 16.9$ kcal/mol. As expected, entropy does play an important role in facilitating the kinetics of the hydrolysis.

Bimolecular Hydrolysis of Benzenediazonium Ion. Pre- and Postcoordination. We found a small theoretical level dependency of the symmetry of the precoordination complex, **4** (Figure 1). At the RHF and MP2 levels, the structure of the precoordination complex is **4a**, with the O atom located in the symmetry plane. In the optimized structure **4b** obtained at the B3LYP level, the water is slightly out of the plane of the benzenediazonium ion. In both cases, the water forms a loose complex with **1** by way of a hydrogen-bond-like interaction with an ortho-hydrogen atom and by the interaction with the positively charged N_2 . We discussed “incipient nucleophilic attack” on diazonium ions in detail and the geometries of **4** are further examples of this theme.³⁵ The O–H distance of the “hydrogen-bond” is 2.3–2.4 Å, and the O–N distances are 2.8–2.9 Å. The bonding in the precoordination complex is substantial with $\Delta E = 14.5$ kcal/mol, $\Delta H = 12.3$ kcal/mol, and $\Delta G = 4.2$ kcal/mol.

Experimental studies in argon matrix³⁶ and in supersonic expansions³⁷ and theoretical studies³⁸ of the benzene–water complex have shown that the water molecule is located above the benzene ring with the O atom on the C_6 axis of the benzene ring with the two H atoms pointing toward benzene. Mons et al.^{37g} found the equilibrium structure of the water complex of benzene cation to be significantly different from the water complex of benzene. In the water complex of benzene cation, the O atom of water can either be in the benzene plane and interact with two neighboring H atoms of the benzene cation

Scheme 3. Approach Path Options



or reside on the C_6 axis of benzene with two H atoms pointing to the opposite direction of the benzene π -cloud.^{38f} They further explained that the reason for this change of location of the water molecule is that the repulsive electrostatic interaction of the charged benzene molecule with the permanent dipole of water, around 10 kcal/mol, overcomes the attractive interactions (dispersion and polarization interactions) totaled up to 9.2 kcal/mol. The structure of **4** can be understood by the reason provided by Mons et al.^{37g} We also searched for a structure in which water is above the benzene ring, but such structures apparently do not correspond to local minima. We considered the post-coordination complex **5** in which dinitrogen is bonded to one of the OH bonds (Figure 1). Solca and Dopfer recently provided experimental evidence for such structures in the gas phase.³⁹

S_N2Ar Transition State Structures. We considered two options for the water molecule to attack benzenediazonium ion (Scheme 3). The planar attack (denoted by “ip”) has the water entering with its O atom in the plane of the benzene ring, while in the out-of-plane attack (denoted by “oop”) the water approaches from above the plane.

Cuccovia et al.¹⁶ reported two RHF/6-31+G* transition state structures, one for in-plane and one for out-of-plane attack, and the out-of-plane structure is more stable than the planar structure by 2.2 kcal/mol. In the present work, we found that the optimization of the transition state structure is theory-dependent. The optimized transition state structures at the three theoretical levels are shown in Figure 2. At the RHF level, only the planar C_s -**TS1a** is a transition state structure (70.7i cm^{-1}) with a relative energy of 10.7 kcal/mol. The out-of-plane C_s structure **TS1b** is a second-order saddle point (97.7i, 23.9i cm^{-1}). The displacement vector analysis shows that the second imaginary mode represents the out-of-plane vibration of the water molecule. The RHF/6-31G** calculations thus indicate one transition state structure, while Cuccovia et al. reported two transition state structures on the RHF/6-31+G* potential energy surface. At the MP2 level, we again only found one transition state structure (185.5i cm^{-1}), but at this level it is the out-of-plane C_s structure, **TS2b**, with a relative energy of 19.3 kcal/mol. The planar C_s structure **TS2a** is a second-order saddle point (98.4i, 15.2i cm^{-1}), and the second imaginary frequency corresponds to the bending of water in and out of the symmetry plane. The B3LYP transition state structure searches led to two structures, and these are the planar C_s and the out-of-plane C_1 structures **TS3a** (103.7i cm^{-1}) and **TS3c** (205.4i cm^{-1}), respectively. **TS3c** is favored over **TS3a** by 0.8 kcal/mol. The out-of-plane C_s structure **TS3b** has two imaginary modes (187.5i, 75.7i cm^{-1}). The second imaginary mode corresponds to the O–H out-of-plane vibration.

The search for the S_N2Ar transition state structures shows that the structure of the transition state depends on the theoretical level. Furthermore, it is found that methods with electron correlation (MP2) tend to give out-of-plane transition state

(34) Shultz, G.; Portalone, G.; Ramondo, F.; Domenicano, A.; Hargittai, I. *Struct. Chem.* **1996**, *7*, 59.

(35) (a) Glaser, R.; Horan, C. J. *Can. J. Chem.* **1996**, *74*, 1200. (b) Horan, C. J.; Barnes, C. L.; Glaser, R. *Chem. Ber.* **1993**, *126*, 243. (c) Glaser, R.; Mummert, C. L.; Horan, C. J.; Barnes, C. L. *J. Phys. Org. Chem.* **1993**, *6*, 201. (d) Horan, C. J.; Haney, P. E.; Barnes, C. L.; Glaser, R. *Acta Crystallogr.* **1993**, *C49*, 1525. (e) Horan, C. J.; Barnes, C. L.; Glaser, R. *Acta Crystallogr.* **1993**, *C49*, 507. (f) Glaser, R.; Horan, C. J.; Nelson, E.; Hall, M. K. *J. Org. Chem.* **1992**, *57*, 215.

(36) Engdahl, A.; Nelander, B. *J. Phys. Chem.* **1985**, *89*, 2860.

(37) (a) Gord, J. R.; Garrett, A. W.; Severance, D. L.; Zwier, T. S. *Chem. Phys. Lett.* **1991**, *178*, 121. (b) Gotch, A. J.; Zwier, T. S. *J. Chem. Phys.* **1992**, *96*, 3388. (c) Pribble, R. N.; Garrett, A. W.; Haber, K.; Zwier, T. S. *J. Chem. Phys.* **1995**, *103*, 531. (d) Suzuki, S.; Green, P. G.; Bumgarner, R. E.; Dasgupta, S.; Goddard, W. A., III; Blake, G. A. *Science* **1992**, *257*, 942. (e) Dasgupta, S.; Smith, K. A.; Goddard, W. A., III. *J. Phys. Chem.* **1993**, *97*, 1081. (f) Gutowsky, H. S.; Emilsson, T.; Arunan, E. *J. Chem. Phys.* **1993**, *99*, 4883. (g) Courty, A.; Mons, M.; Dimicoli, I.; Piuze, F.; Gaigeot, M.; Brenner, V.; Pujol, P. D.; Millié, P. *J. Phys. Chem. A* **1998**, *102*, 6590.

(38) (a) Linse, P.; Karlström, G.; Jönsson, B. *J. Am. Chem. Soc.* **1993**, *99*, 4483. (b) Brédas, J. L.; Street, G. B. *J. Chem. Phys.* **1989**, *90*, 7291. (c) Cheney, B. V.; Schultz, M. W.; Cheney, J.; Richards, W. G. *J. Am. Chem. Soc.* **1988**, *110*, 4195. (d) Cheney, B. V.; Schultz, M. W. *J. Phys. Chem.* **1990**, *94*, 6228. (e) Augspurger, J. D.; Dykstra, C. E.; Zwier, T. S. *J. Phys. Chem.* **1992**, *96*, 7252. (f) Gregory, J. K.; Clary, D. C. *Mol. Phys.* **1996**, *88*, 33.

(39) Solca, N.; Dopfer, O. *J. Am. Chem. Soc.* **2004**, *126*, 1716.

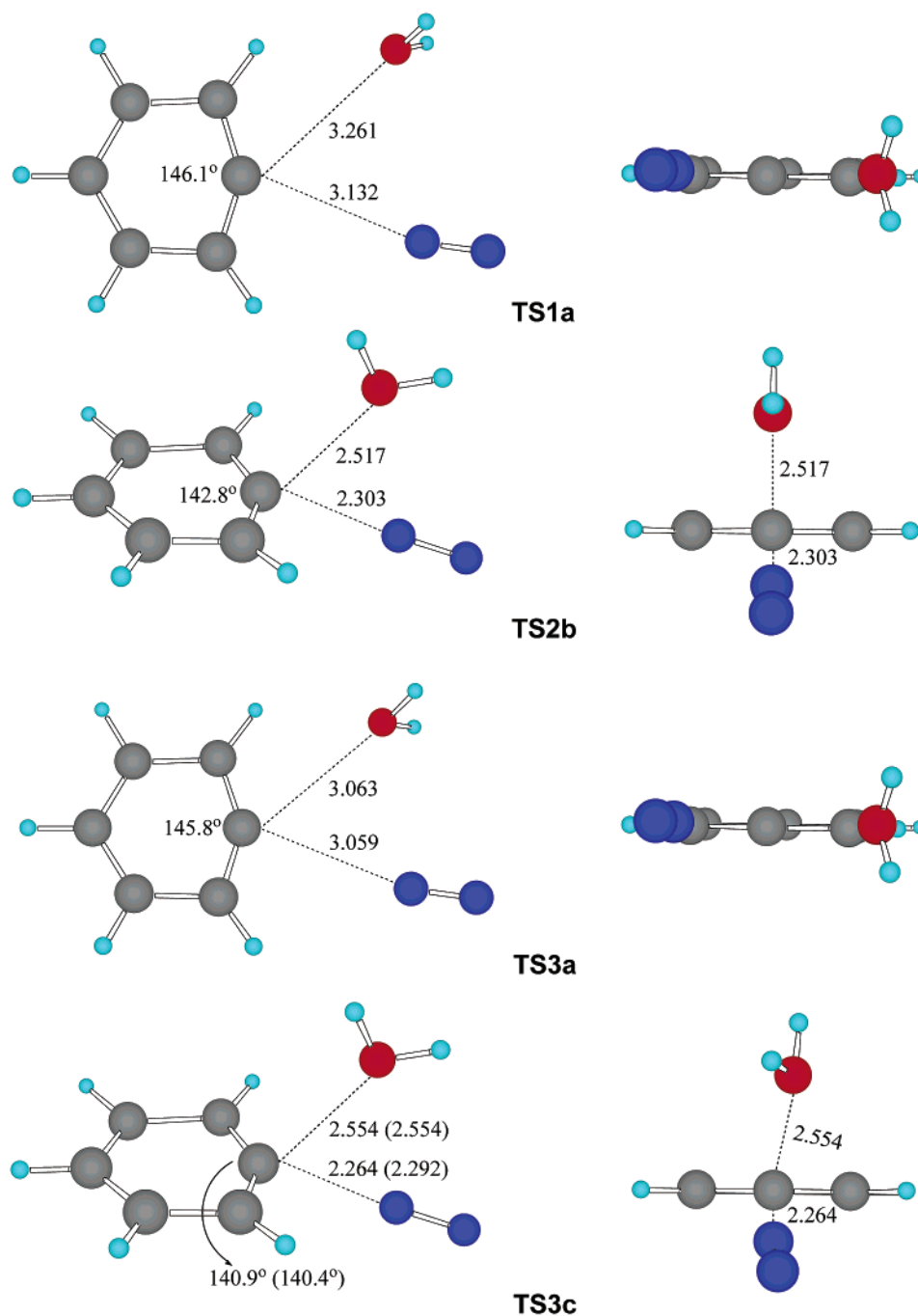


Figure 2. Transition state structures **TS**. Numbers indicate the method of optimization (1 = RHF, 2 = MP2, 3 = B3LYP) and letters indicate the topology and symmetry (a = ip and C_s , b = oop and C_s , c = oop and C_1). Values given in parentheses for **TS3c** refer to **TS3b**. The online version contains a web-enhanced object showing an animation of the transition vector of **TS2b**.

structures, while methods without electron correlation (RHF) tend to give planar transition state structures. The B3LYP calculation found both out-of-plane and planar first-order saddle points. QCISD(T)/6-31G**/B3LYP/6-31G** and QCISD(T)/6-31G**/MP2(full)/6-31G** single-point energy calculations confirmed that **TS3c** is more stable than **TS3a** by 0.8 kcal/mol, respectively, and that **TS2b** is 1.0 kcal/mol more stable than **TS2a**, respectively. Therefore, **TS2b** is likely to be the preferred transition state structure for the bimolecular reaction, and energy penalties are small for any twist between the best common plane of the nucleophiles and the benzene plane.⁴⁰

TS2b and **TS3c** both feature CN contacts of 2.3 Å and CO contacts of 2.5 Å. **TS1a** and **TS3a**, the planar structures, have

long CN distances of 3.1 Å and CO distances up to 3.3 Å. Because of these distances, the energy difference between ip- and oop-type structures are small at any level, and the theoretical level dependencies are therefore not surprising. *The characteristic feature that matters most is that the transition state structures for the bimolecular reaction all are rather loose.*

The S_N2Ar transition state structure features a phenyl cation interacting weakly with water and dinitrogen. Hence, the electronic relaxations associated with dediazonation essentially are the same in the S_N1Ar and S_N2Ar processes.

(40) It is very likely that the preference for **TS2b** increases as a result of specific solvation; see the discussion of the precoordination complexes.

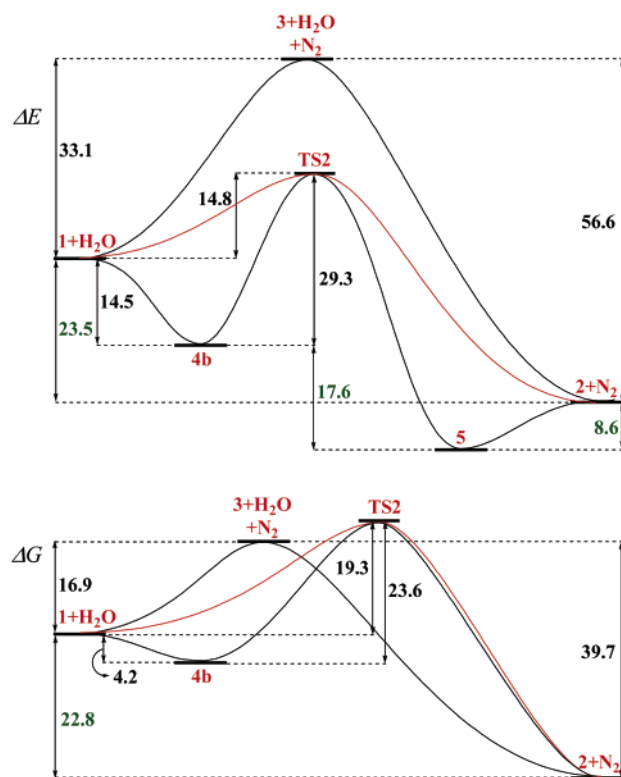


Figure 3. Potential energy and Gibbs free energy diagrams for the reaction of benzenediazonium ion with one water molecule (QCISD(T)/MP2 level).

Comparison of the S_N1Ar , S_N2Ar , and Direct S_N2Ar Reactions. The potential energy and Gibbs free energy diagrams of the reaction of water with benzenediazonium ion are shown in Figure 3 and they illustrate two important results. At the QCISD(T)/MP2 level, we find activation enthalpies of $\Delta H^\ddagger = 28.3$ kcal/mol for the S_N1Ar process and $\Delta H^\ddagger = 25.9$ kcal/mol for the S_N2Ar reaction. The bimolecular path is favored by 2.4 kcal/mol, and this is the expected result. However, the S_N1Ar activation Gibbs free energy $\Delta G^\ddagger = 16.9$ kcal/mol is much less than the S_N2Ar value of $\Delta G^\ddagger = 23.6$ kcal/mol. Hence, the calculations show that the unimolecular reaction of water with benzenediazonium ion is preferred over the bimolecular reaction by $\Delta G^\ddagger = 6.7$ kcal/mol, and this result is probably less expected. The entropy change associated with the unimolecular path helps to lower the overall ΔG^\ddagger by almost 10 kcal/mol, and this is large enough to make the unimolecular process the preferred one.

In hydrolyses, the strict S_N1Ar reaction is not possible, because there will always be a certain pressure of water molecules and the C–N dissociation can never evolve to completion. The nucleophilicity of water in water is less than that of an isolated water molecule, but the affinity of one water toward an incipient cation will always greatly exceed the affinity of one water to any number of water molecules. Hence, there is no opportunity for the phenyl cation to exist ever in a water cage, and in hydrolysis reactions the “unimolecular mechanism” actually *has to involve the reacting solvent molecule*, and we propose that the best model for this reaction is the S_N2Ar reaction model. Hence, the computed activation parameters for the S_N2Ar model reaction of water with benzenediazonium ion are the most relevant data with regard to the hydrolysis of benzenediazonium ion. The reaction with water in a less nucleophilic solvent (e.g. dilute mineral or carboxylic acids)

also does not allow for complete C–N dissociation, because one solvent molecule inevitably will bind to the incipient phenyl cation, and this binding ($3 \cdot \text{solvent}$) will occur in concert with the dissociation for the very same reason as above. In this case, the hydrolysis becomes a sequence of reactions via $3 \cdot \text{solvent}$. The S_N1Ar reaction would require the formation of solvated 3 *without* specific solvent interaction in the transition state, and that is not possible.

Above, we computed the activation parameters for S_N2Ar reaction based on the energies of the aggregate $1 \cdot \text{H}_2\text{O}$ and the transition state structure. However, in the solvolysis of benzenediazonium ion, the solvating water and the reactive water will not be the same. Even in the gas phase, the reaction of one water with benzenediazonium ion bypasses the deep potential energy minimum of the precoordination complex because of the reaction dynamics,⁴¹ and similar observations have been reported.^{42,43} The direct S_N2Ar model reaction *without* precoordination (red line in Figure 3) is characterized by activation parameters of $\Delta H^\ddagger = 13.6$ kcal/mol and $\Delta G^\ddagger = 19.3$ kcal/mol. To ascertain the validity of these computed data, we examined their convergence with regard to an improvement in the basis set. It is reassuring that the QCISD(T)/6-311G(2df,p) enthalpy of 15.1 kcal/mol closely agrees with the QCISD(T)/6-31G** data (Table 1).

On the basis of the direct S_N2Ar model, we have to conclude that the measured activation enthalpy of 27 ± 1 kcal/mol is about 12 kcal/mol higher as compared to our best computed value for the model reaction in a vacuum. Even though the S_N1Ar and S_N2Ar models provide activation enthalpies that very closely match the experimental value (S_N1Ar , 28.3 kcal/mol; S_N2Ar , 25.9 kcal/mol), our analysis leads to the unavoidable conclusion that this agreement is fortuitous. Hence, the experiments show that the solvent effect on the activation energy is about the same for all solvents, and the experimental data in combination with the present computed data suggest that the solvent effect on the dediazonation is approximately 12 kcal/mol.

Secondary Kinetic Hydrogen Isotope Effects. In a seminal paper, Swain et al.⁴⁴ measured secondary kinetic isotope effects for a variety of 2-, 4-, 3,5-, and 2,4,6-deuterated benzenediazonium fluoborates in dilute mineral and carboxylic acids. These data are consistent with a rather complete C–N dissociation in the rate-limiting step and supported the S_N1Ar mechanism. We computed SKIE values for the reactions $1 \rightarrow 3$ (S_N1Ar) and $1 \rightarrow \text{TS2}$ (direct S_N2Ar) for the 2-, 3-, and 4-deuterated species (Table 2). The experimental data show solvent effects on the SKIE of about 0.03. Since specific solvation is largest for the ortho-H, any such solvent effect should be manifested most strongly for the ortho SKIE. Nevertheless, the agreement between the experimental data and the computed gas phase data is remarkably good. Most importantly, the data in Table 2 clearly show that the SKIE does not allow for a distinction between S_N1Ar and S_N2Ar reactions. In particular, the “total agreement” between the

(41) Wu, Z.; Glaser, R., to be published.

(42) Sun, L.; Song, K.; Hase, W. L. *Science* **2002**, 296, 875.

(43) See also: (a) Mann, D. J.; Hase, W. L. *J. Am. Chem. Soc.* **2002**, 124, 3208. (b) Nummela, J. A.; Carpenter, B. K. *J. Am. Chem. Soc.* **2002**, 124, 8512. (c) Ammal, S. C.; Yamataka, H.; Aida, M.; Dupuis, M. *Science* **2003**, 299, 1555.

(44) Swain, C. G.; Sheats, J. E.; Gorenstein, D. G.; Harbison, K. G. *J. Am. Chem. Soc.* **1975**, 97, 791.

Table 3. Computed Solvent Effects on Pertinent Relative, Reaction, and Activation Energies^{a,b}

	water			methanol		
	ΔE_{sol}	ΔH_{cond}	ΔG_{cond}	ΔE_{sol}	ΔH_{cond}	ΔG_{cond}
1 → Ph ⁺ + N ₂	-4.1	30.4	19.0	-4.1	30.4	19.1
Ph ⁺ + H ₂ O → 2	-8.0	-62.5	-51.1	-7.7	-62.2	-50.7
1 + H ₂ O → 1 ·H ₂ O	10.5	-2.2	5.8	10.2	-2.5	5.6
1 + H ₂ O vs TS	7.0	25.1	30.9	6.9	25.0	30.8
1 ·H ₂ O vs TS	-3.4	27.4	25.1	-3.3	27.5	25.2
1 + H ₂ O → 2 + N ₂	-12.1	-32.3	-32.0	-11.7	-31.9	-31.7
	CF ₃ CH ₂ OH			DMSO		
	ΔE_{sol}	ΔH_{cond}	ΔG_{cond}	ΔE_{sol}	ΔH_{cond}	ΔG_{cond}
1 → Ph ⁺ + N ₂	-4.0	30.5	19.1	-4.1	30.4	19.1
Ph ⁺ + H ₂ O → 2	-7.6	-62.1	-50.7	-7.9	-62.4	-50.9
1 + H ₂ O → 1 ·H ₂ O	10.1	-2.6	5.5	10.3	-2.4	5.7
1 + H ₂ O vs TS	6.8	24.9	30.7	7.0	25.1	30.8
1 ·H ₂ O vs TS	-3.3	27.5	25.2	-3.4	27.4	25.1
1 + H ₂ O → 2 + N ₂	-11.6	-31.8	-31.5	-11.9	-32.1	-31.8
	water ^c			water ^d		
	ΔE_{sol}	ΔH_{cond}	ΔG_{cond}	ΔE_{sol}	ΔH_{cond}	ΔG_{cond}
1 → Ph ⁺ + N ₂	-4.1	24.2	12.8	-4.1	25.9	14.5
Ph ⁺ + H ₂ O → 2	-8.0	-59.2	-47.7	-8.0	-60.5	-49.0
1 + H ₂ O → 1 ·H ₂ O	10.5	-1.8	6.3	10.5		
1 + H ₂ O vs TS	7.0	20.6	26.3	7.0	22.1	27.8
1 ·H ₂ O vs TS	-3.4	22.5	19.1	-3.4		
1 + H ₂ O → 2 + N ₂	-12.1	-35.1	-34.9	-12.1	-37.7	-34.5

^a All data in kcal/mol. ^b IPCM calculations at the MP2/6-31G** level. ^c Based on QCISD(T)/6-31G**//MP2/6-31G** energies. ^d Based on QCISD(T)/6-311G(2df,p)//MP2/6-31G** energies.

computed and measured SKIE of the 2-deuterated species does not present any better evidence for the S_N1Ar reaction than does the “total agreement” of the computed and measured SKIE of the 3-deuterated species in favor of the S_N2Ar reaction. It is precisely for the great similarities of the phenyl cation moiety in the S_N1Ar and S_N2Ar reactions that the isotope studies did not alert anybody that S_N1Ar might not be operative.

IPCM Computation of Solvation Effects. The deductions made on the basis of the ab initio studies are corroborated by the results of IPCM calculations for four representative solvents (Table 3): water ($\epsilon = 78.3$), methanol ($\epsilon = 32.6$), 2,2,2-trifluoroethanol ($\epsilon = 27.7$), and DMSO ($\epsilon = 46.7$).

The computed solvation data show that the solvent effects (ΔE_{sol}) are virtually independent of the solvent, and this result

is in agreement with the experimental observations.^{30b,c} Can this solvent independence can be explained on the basis of the electron density relaxation associated with dissociation,¹⁴ and it is true for both the S_N1Ar and the direct S_N2Ar model reactions?

The data show that solvation decreases the activation energy for the S_N1Ar by about 4 kcal/mol, while it increases the activation energy for the direct S_N2Ar by about 7 kcal/mol. The data at the bottom of Table 3 combine these solvation corrections with the thermochemical data computed at the same level and the QCISD(T) energy data. The overall agreement between the experimental data and the computed dissociation energy is not meaningful, even though it is “excellent”. On the other hand, the solvation effects provide for much better numerical agreement between the experimental value of 27 ± 1 kcal/mol and the conceptually meaningful S_N2Ar activation barrier of 22.1 kcal/mol. In fact, this agreement is encouraging and we hope to achieve even better agreement in future studies that account for specific solvation effects as well.

Conclusion

It is likely that many chemists intuitively think of the very loose S_N2Ar mechanism when they refer to the “unimolecular mechanism” in solution. Our contribution therefore merely consists of the precise statement of the conceptual differences between these processes. This conceptual clarity allows for two major conclusions. The S_N2Ar reaction provides a more realistic model for mechanistic discussions of the dediazonation of aromatic diazonium ions than the consideration of the S_N1Ar reaction. The analysis reveals that the agreement between computed gas phase S_N1Ar activation enthalpies and activation barriers measured in solution is fortuitous. While the solvent effect on dediazonations is essentially independent of the solvent, the solvent effect on dediazonations is substantial and it is reaction-rate-retarding.

Acknowledgment. This research was supported by the National Institutes of Health (GM61027).

Supporting Information Available: Tables with total energies and Cartesian coordinates of optimized structures. This material is available free of charge via the Internet at <http://pubs.acs.org>.

JA047620A